Received September 14, 2019, accepted October 5, 2019, date of publication October 15, 2019, date of current version November 1, 2019.

Digital Object Identifier 10.1109/ACCESS.2019.2947455

The Bearing-Only Target localization via the Single UAV: Asymptotically Unbiased Closed-Form Solution and Path Planning

LANG HE[1,3], PAN GONG[1,3], XIAOFEI ZHANG[1,2,3], AND ZHENG WANG[1,3], (Member, IEEE)

[1]Key Laboratory of Dynamic Cognitive System of Electromagnetic Spectrum Space, Ministry of Industry and Information Technology, Nanjing University of Aeronautics and Astronautics, Nanjing 210007, China

[2]State Key Laboratory of Millimeter Waves, Southeast University, Nanjing 210000, China

[3]Department of Electrical and Information Engineering, Nanjing University of Aeronautics and Astronautics, Nanjing 210007, China

Corresponding author: Xiaofei Zhang (zhangxiaofei@nuaa.edu.cn)

This work was supported in part by the China NSF under Grant 61971217 and Grant 61601167, in part by the Open Research Fund of State Key Laboratory of Millimeter Waves, Southeast University, under Grant K201826, in part by the Open Research Fund of State Key Laboratory of Complex Electromagnetic Environment Effects on Electronics and Information System under Grant CEMEE2019Z0104B, and in part by the Fundamental Research Funds for the Central Universities under Grant NE2017103 and Grant NT2019013.

ABSTRACT The target localization based on the unmanned aerial vehicle (UAV) is becoming more and more popular due to its flexible mobility. In this paper, the bearing-only localization with respect to the single UAV in the three-dimensional (3D) scenario is studied by the angle of arrival (AOA). In the current researches, the bias of the closed-form solution caused by the coefficient errors of the pseudo-linear equations constructed by the AOA is not effectively eliminated. In order to reduce the bias, an asymptotically unbiased localization algorithm is proposed, which eliminates the bias by constructing the constrained weighted least-squares. Since the term that causes the bias is constrained to a constant, which no longer affects the closed-form solution of the pseudo-linear equations, the closed-form solution is unbiased. After that, the position errors of the UAV are considered in path planning, which improves localization accuracy by taking account of both AOA errors and position errors of the UAV rather than just AOA errors.

INDEX TERMS Path planning, target localization, AOA, UAV.

I. INTRODUCTION

A. BACKGROUND AND MOTIVATION

Recently, the bearing-only target localization has been an important research topic in various fields. Different from the time difference of arrival (TDOA) and frequency difference of arrival (FDOA), the AOA-based target localization does not require the time and frequency synchronization, which makes it suitable to use the single UAV for non-cooperative localization [1]–[3]. However, there are still some problems in current researches. Firstly, the closed-form solution of the pseudo-linear equation constructed by AOA is still biased due to the nonlinear relation between the AOA errors and the coefficient errors of pseudo-linear equation [4]–[8]. Secondly, the position errors of the UAV have not been considered in the path planning [9]–[12], which also degrades the localization accuracy.

The associate editor coordinating the review of this manuscript and approving it for publication was Xianpeng Wang.

B. RELATED WORK

Due to the nonlinear relation between the AOA measurements and the target position [13]–[16], it is difficult to directly solve the target position with the knowledge of AOA. Reference [17] estimated the target position by the Gauss-Newton implementation of the Maximum Likelihood Estimator (MLE). In addition to the high computational complexity, its localization performance severely suffers from the initial estimate. A pseudo linear estimator (PLE) with the closed-form solution in the two-dimensional (2D) scenario was proposed to reduce computational complexity and overcome the effect of the initial estimate [18]. Nevertheless, the bias caused by the coefficient errors of the pseudo-linear equations is not considered in the closed-form solution of PLE. There were some attempts based on the instrumental variable (IV) estimator to reduce the bias of the PLE [15], [19]–[21]. These IV estimators fail to provide a closed-form solution due to the iterative procedures. In order to develop an estimator without iterative procedures, a closed-form asymptotically unbiased IV estimator was proposed in [22]. However, the above-mentioned researches only considered the 2D scenario, while there are still many intractable problems for the target localization in three-dimensional (3D) geometries. Recently, a few literatures have investigated the target localization in the 3D scenario [23]–[25]. Considering that the bias of target localization methods is influenced by the coefficient errors of pseudo-linear equations, a novel bias reduction pseudo-linear estimator (BRPLE) was developed to reduce the bias [26]. However, the bias caused by the coefficient errors of the pseudo-linear equation is not effectively eliminated because the term that causes the bias is very difficult to calculate.

On the other hand, the trajectory of the UAV plays an important role in the path planning [27]–[29]. Specifically, the localization accuracy of different trajectories can be characterized by the Cramer-Rao lower bound (CRLB), which is the inverse matrix of the Fisher information matrix (FIM) [30]. In the context of bearings-only target motion analysis, maximizing the determinant of FIM is preferred as the criteria of the path planning [11], [31]–[33]. In order to develop a more realistic system model, the scenario of obstacles and no-fly zones was considered in [34], [35]. All these papers simply assume that the position of the UAV is completely accurate. In fact, the position of the UAV usually obtained by the global position system (GPS) in practice is not accurate. The coefficient errors of the pseudo-linear equation increase due to the influence of both the errors of measurement angles and the position errors of the UAV, which degrades the localization performance. So it is necessary to consider the impact of both AOA errors and position errors of the UAV in path planning. To the best knowledge of the authors, current researches on path planning have not considered the position errors of the UAV.

C. CONTRIBUTIONS

In this paper, the improved BRPLE (IBRPLE) is proposed to reduce the bias of closed-form solution in the pseudo-linear equation. The closed-form solutions of the pseudo-linear equations in [23], [24], [26] are based on the weighted least squares solution. Although the closed-form solution does not require the initial estimate, it is always biased because the term that causes the bias is very difficult to calculate. In this paper, the bias will be reduced from two aspects in this paper. On the one hand, the weight of the equation constructed by the elevation angle was calculated by only considering the elevation-angle errors in [26], which is recalculated by considering the azimuth errors, the elevation-angle errors and the position errors of the UAV. On the other hand, we divide the cost function based on the weighted least squares into two parts. The first part contains the parameters to be estimated and the real value of the pseudo linear equation coefficients, and the second part consists of the parameters to be estimated and the coefficient errors caused by the AOA measurements and the position measurements.

The bias of closed-form solution is mainly caused by the second part. The ideal of reducing the bias is that the minimum of the cost function is determined by the first part if the second part is equal to a constant. Hence the cost function can achieve the minimum at the ideal solution and the solution is unbiased because the first part is the real coefficients of the pseudo linear equation. In practice, the second part is equal to a constant that will be used as a constraint of the cost function to construct a constrained weighted least squares problem. This problem will be solved by Lagrangian multiplier method. In practice, the coefficient errors should be known when the second part is used as a constraint. However, it is impossible to calculate the coefficient errors accurately because they are caused by the random measurement errors. They will be calculated by the statistical method. Meanwhile, how to calculate the expectation of coefficient errors with higher precision is also a challenge due to nonlinear relation between the random measurement errors and the coefficients of pseudo-linear equations. In the section III, the method will be proposed to calculate the expectation of coefficient errors with higher precision, which will improve the localization performance significantly.

In order to improve the accuracy of localization through adjusting the position of UAV, a path planning algorithm considering the position error of the UAV is proposed in this paper. Maximizing the determinant of FIM is the criterion for the path planning of the UAV. We assume that the position of the UAV is not accurate. It is obvious that the position of the UAV is also the parameter to be estimated like the speed and position of the target. The FIM of all parameters to be estimated is easily calculated. However, the FIM of the initial position and speed of the target is what we really want to calculate because they are the parameters that we hope to estimate with the high precision, which is calculated by the relation between FIM and CRLB from the FIM of all parameters to be estimated.

To summarize the contributions in this paper, they are summarized as follows:

- By taking into account the measurement errors of azimuth-angle, elevation-angle, and the position of the UAV, the improved weighting matrix for the weighted least squares (WLS) estimator is calculated. On this basis, an asymptotically bias-reduced closed-form solution of the proposed IBRPLE is obtained by solving the constructed constrained weighted least-squares problem. Compared with other localization algorithms, the proposed IBRPLE algorithm can obtain higher localization accuracy because it reduces the bias of nonlinear equations.
- Based on the determinant maximization criterion of FIM, an effective UAV path planning scheme is developed to further improve the localization accuracy of the

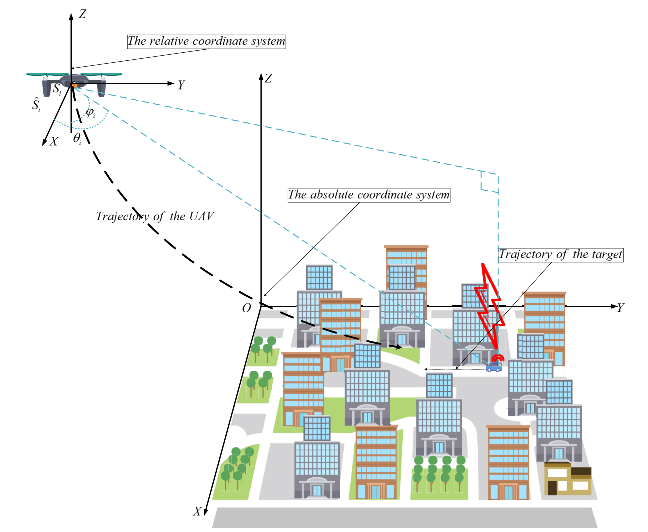

FIGURE 1. The system model based on the single UAV in the 3D scenario.

proposed UAV assisted bearing-only target localization algorithm, while also considering the estimated errors of the position of the UAV. By considering the position errors of the UAV in the cost function of the path planning, the path planning algorithm proposed in this paper can achieve higher localization accuracy.

- The performance of the UAV assisted bearing-only 3D target localization is characterized by simulation results, and other classical localization methods are also provided for comparison. Simulations show the validity of analytical results and the superiority of the proposed IBRPLE to other estimators. The designed UAV path planning scheme is also verified by corresponding simulations and it is shown the path planning with measurement errors taken into account can bring about the improvement of localization accuracy.

D. ORGANIZATION

This paper is organized as follows. The system model for localization with a moving target in the 3D scenario is given in Section II. The asymptotically unbiased closed-form solution for the AOA localization will be derived in Section III. In Section IV, the path planning algorithm of the UAV is also proposed under the position errors of the UAV. In section V, the simulations are carried out and corresponding comparisons with other algorithms are also provided. In section VI, conclusions are drawn.

Notation: In this paper, $\hat{\cdot}$ represents the measured value. $\det(\cdot)$ is the determinant of a matrix. $E\{\cdot\}$ is the statistical expectation of a random variable. $\mathbf{0}_{mn}$ is the $m\times n$ zero matrix. $\boldsymbol{I}_m$ is the $m \times m$ unit matrix.

II. SYSTEM MODEL FOR 3D MOVING TARGET

In this section, we consider a system model for the 3D moving target localization based on the single UAV. This model assumes that the target moves linearly at a constant velocity $\boldsymbol{v}_t = [v_x, v_y, v_z]^T$. As shown in Fig.1, the relative coordinate system is established to describe the AOA from the target to the UAV, whose axes are parallel to the axes of the absolute coordinate system and coordinate origin is set to the position of the UAV. The position vectors of the UAV and the target are described in the absolute coordinate system, which are denoted as $\boldsymbol{s} = [\boldsymbol{s}_0^T, \boldsymbol{s}_1^T, \ldots, \boldsymbol{s}_{N-1}^T]^T$ and $\boldsymbol{p} = [\boldsymbol{p}_0^T, \boldsymbol{p}_1^T, \ldots, \boldsymbol{p}_{N-1}^T]^T$, respectively, where N is the total number of AOA measurements, $\boldsymbol{s}_i = [x_i, y_i, z_i]^T$ is the position of the UAV at the ith measurement and $\boldsymbol{p}_i = [x_{ti}, y_{ti}, z_{ti}]^T$ is the position of the target at the ith measurement. The interval between adjacent AOA measurements is assumed to be a constant T. In fact, the position vector of the UAV measured by the GPS is imprecise, whose measurement is given as

$$\hat{\boldsymbol{s}} = \boldsymbol{s} + \Delta\boldsymbol{s}, \tag{1}$$

where $\Delta\boldsymbol{s} = [\Delta\boldsymbol{s}_0^T, \Delta\boldsymbol{s}_1^T, \ldots, \Delta\boldsymbol{s}_{N-1}^T]^T$ is a Gaussian vector with zero mean and covariance matrix $\boldsymbol{Q}_s$, where $\Delta\boldsymbol{s}_i = [\Delta x_i, \Delta y_i, \Delta z_i]^T$ is the position error of the UAV at the ith measurement.

Consequently, the real azimuth angle θ_i and elevation angle φ_i at the ith measurement can be expressed as

$$\theta_i = \arctan\left(\frac{y_{ti} - y_i}{x_{ti} - x_i}\right), \tag{2a}$$

$$\varphi_i = \arctan\left(\frac{z_{ti} - z_i}{(x_{ti} - x_i)\cos(\theta_i) + (y_{ti} - y_i)\sin(\theta_i)}\right), \tag{2b}$$

where $\theta_i \in (-\pi, \pi]$ and $\varphi_i \in (-\pi/2, \pi/2]$. For writing convenience, the real azimuth angle vector and the elevation angle vector are denoted as $\boldsymbol{\theta} = [\theta_0, \theta_1, \ldots, \theta_{N-1}]^T$ and $\boldsymbol{\varphi} = [\varphi_0, \varphi_1, \ldots, \varphi_{N-1}]^T$, respectively. In practice, the measurements of the azimuth angle vector and the elevation angle vector are obtained by the UAV, which have errors due to the jitter of the UAV or the noise of the wireless channel, and they can be written as

$$\hat{\boldsymbol{\theta}} = \boldsymbol{\theta} + \boldsymbol{n}, \tag{3a}$$

$$\hat{\boldsymbol{\varphi}} = \boldsymbol{\varphi} + \boldsymbol{\omega}, \tag{3b}$$

where $\boldsymbol{n} = [n_0, n_1, \ldots, n_{N-1}]^T$ and $\boldsymbol{\omega} = [\omega_0, \omega_1, \ldots, \omega_{N-1}]^T$ are the zero-mean Gaussian noises with covariance matrices $\boldsymbol{Q}_n$ and $\boldsymbol{Q}_\omega$, respectively. The covariance matrices for AOA measurements have the following forms:

$$\boldsymbol{Q}_{\boldsymbol{n}} = \begin{bmatrix} \sigma_0^2 & & 0 \\ & \ddots & \\ 0 & & \sigma_{N-1}^2 \end{bmatrix} = \sigma_n^2 \begin{bmatrix} d_0^\lambda & & 0 \\ & \ddots & \\ 0 & & d_{N-1}^\lambda \end{bmatrix}, \tag{4a}$$

$$\boldsymbol{Q}_{\boldsymbol{\omega}} = \begin{bmatrix} \rho_0^2 & & 0 \\ & \ddots & \\ 0 & & \rho_{N-1}^2 \end{bmatrix} = \sigma_\omega^2 \begin{bmatrix} d_0^\lambda & & 0 \\ & \ddots & \\ 0 & & d_{N-1}^\lambda \end{bmatrix}, \tag{4b}$$

where σ_n^2 and σ_ω^2 are the reference variances of the azimuth angle and elevation angle at unit range, $\lambda (0 \le \lambda < 2)$ is the power loss exponent [35], $d_i = \|\boldsymbol{p}_i - \boldsymbol{s}_i\|$ is the distance from the target to the UAV at the ith measurement, σ_i^2 is the variance of azimuth angle at the ith measurement and ρ_i^2 is the variance of elevation angle at the ith measurement.

The goal of target localization is to find the last position of $\boldsymbol{p}_i$, which is difficult to be estimated by directly using multiple measurements. However, since the target moves linearly at a constant velocity [36], the position $\boldsymbol{p}_i$ can be written as

$$\boldsymbol{p}_i = \boldsymbol{p}_0 + iT\boldsymbol{v}_t = \boldsymbol{M}_i\boldsymbol{x}, \tag{5}$$

where $\boldsymbol{x} = [\boldsymbol{p}_0^T, \boldsymbol{v}_t^T]^T$ and

$$\boldsymbol{M_i} = \begin{bmatrix} 1 & 0 & 0 & iT & 0 & 0 \\ 0 & 1 & 0 & 0 & iT & 0 \\ 0 & 0 & 1 & 0 & 0 & iT \end{bmatrix}. \tag{6}$$

Therefore, the last position of $\boldsymbol{p}_i$ can be obtained indirectly by estimating $\boldsymbol{x}$ according to (5). So this paper aims to estimate the vector $\boldsymbol{x}$ as accurate as possible under the measurement vector $\boldsymbol{m} = [\hat{\boldsymbol{\theta}}^T, \hat{\boldsymbol{\varphi}}^T, \hat{\boldsymbol{s}}^T]^T$.

III. THE BIAS REDUCED CLOSED-FORM SOLUTION OF THE 3D MOVING TARGET

In this section, the bias reduced closed-form solution is proposed to improve the localization accuracy. Specifically, we firstly analyse the reason of the bias and the method of reducing bias is given by the constrained weighted least squares method. Subsequently, the weighting matrix used in the method of reducing bias is recalculated by considering the azimuth angle errors, the elevation angle errors and the position errors of the UAV. Finally, the term that causes the bias is calculated by statistical methods.

A. THE BIAS REDUCED CLOSED-FORM SOLUTION

According to (2), the equations constructed by the real azimuth angle θ_i and elevation angle φ_i can be respectively rewritten as

$$\sin(\theta_i)(x_{ti} - x_i) - \cos(\theta_i)(y_{ti} - y_i) = 0, \tag{7a}$$
$$\cos(\theta_i)\sin(\varphi_i)(x_{ti} - x_i) - \sin(\theta_i)\sin(\varphi_i)(y_{ti} - y_i) - \cos(\varphi_i)(z_{ti} - z_i) = 0. \tag{7b}$$

In practice, since there are errors in the AOAs measured by the UAV and the positions of the UAV obtained by GPS, the right of (7) is not always equal to zero. Therefore, μ_i and ν_i are defined as the errors of equations constructed by the AOA measurements and the position measurements of the UAV at the ith measurement [18], which are expressed as

$$\mu_i = \sin(\hat{\theta}_i)(x_{ti} - \hat{x}_i) - \cos(\theta_i)(y_{ti} - \hat{y}_i), \tag{8a}$$
$$\nu_i = \cos(\hat{\theta}_i)\sin(\hat{\varphi}_i)(x_{ti} - \hat{x}_i) - \sin(\hat{\theta}_i)\sin(\hat{\varphi}_i)(y_{ti} - \hat{y}_i) - \cos(\hat{\varphi}_i)(z_{ti} - \hat{z}_i), \tag{8b}$$

Eq.(8) can be simply expressed by vectors as

$$\mu_i = \hat{\boldsymbol{b}}_i^T\boldsymbol{p}_i - \hat{\boldsymbol{b}}_i^T\hat{\boldsymbol{s}}_i, \tag{9a}$$
$$\nu_i = \hat{\boldsymbol{c}}_i^T\boldsymbol{p}_i - \hat{\boldsymbol{c}}_i^T\hat{\boldsymbol{s}}_i, \tag{9b}$$

where $\hat{\boldsymbol{c}}_i = [\cos(\hat{\theta}_i)\sin(\hat{\varphi}_i), \sin(\hat{\theta}_i)\sin(\hat{\varphi}_i), -\cos(\hat{\varphi}_i)]^T$ and $\hat{\boldsymbol{b}}_i = [\sin(\hat{\theta}_i), -\cos(\hat{\theta}_i), 0]^T$. Meanwhile, $\boldsymbol{\eta} = [\mu_0, \mu_1, \cdots, \mu_{N-1}, \nu_0, \nu_1, \cdots, \nu_{N-1}]^T$ is defined as the error vector of the pseudo-linear equations [24], which is obtained by putting (5) into (9) as

$$\boldsymbol{\eta} = \boldsymbol{F}\boldsymbol{x} - \boldsymbol{h}, \tag{10}$$

where

$$\boldsymbol{F} = \begin{bmatrix} \hat{\boldsymbol{b}}_0^T\boldsymbol{M}_0 \\ \hat{\boldsymbol{b}}_1^T\boldsymbol{M}_1 \\ \vdots \\ \hat{\boldsymbol{b}}_{N-1}^T\boldsymbol{M}_{N-1} \\ \hat{\boldsymbol{c}}_0^T\boldsymbol{M}_0 \\ \hat{\boldsymbol{c}}_1^T\boldsymbol{M}_1 \\ \vdots \\ \hat{\boldsymbol{c}}_{N-1}^T\boldsymbol{M}_{N-1} \end{bmatrix}, \quad \boldsymbol{h} = \begin{bmatrix} \hat{\boldsymbol{b}}_0^T\hat{\boldsymbol{s}}_0 \\ \hat{\boldsymbol{b}}_1^T\hat{\boldsymbol{s}}_1 \\ \vdots \\ \hat{\boldsymbol{b}}_{N-1}^T\hat{\boldsymbol{s}}_{N-1} \\ \hat{\boldsymbol{c}}_0^T\hat{\boldsymbol{s}}_0 \\ \hat{\boldsymbol{c}}_1^T\hat{\boldsymbol{s}}_1 \\ \vdots \\ \hat{\boldsymbol{c}}_{N-1}^T\hat{\boldsymbol{s}}_{N-1} \end{bmatrix}. \tag{11}$$

The most closed-form solutions of the pseudo-linear equations in (10) based on the weighted least-squares (WLS) estimator. The inverse of the weighting matrix in the WLS estimator is defined as the covariance matrix of the error vector [30], $\boldsymbol{W}^{-1} = E[\boldsymbol{\eta}\boldsymbol{\eta}^T]$. In [24], the inverse of weighting matrix is approximated as

$$\boldsymbol{W}^{-1} = diag([l_0^2\sigma_0^2 + \sigma_{s0}^2, \ldots, l_{N-1}^2\sigma_{N-1}^2 + \sigma_{s(N-1)}^2, d_0^2\rho_0^2 + \sigma_{s0}^2, \ldots, d_{N-1}^2\rho_{N-1}^2 + \sigma_{s(N-1)}^2]), \tag{12}$$

with $\sigma_{si}^2 = \sigma_{six}^2 = \sigma_{siy}^2 = \sigma_{six}^2$, where σ_{six}^2, σ_{siy}^2 and σ_{siz}^2 are the variances of the three coordinates at the ith measurement position error of the UAV, $l_i = \sqrt{(x_{ti} - x_i)^2 + (y_{ti} - y_i)^2}$ denotes the horizontal distance between $\boldsymbol{p}_i$ and $\boldsymbol{s}_i$ and $d_i = \|\boldsymbol{r}_i\|$ is the distance between $\boldsymbol{p}_i$ and $\boldsymbol{s}_i$, where $\boldsymbol{r}_i = \boldsymbol{p}_i - \boldsymbol{s}_i = d_i[\cos(\theta_i)cos(\varphi_i), \sin(\theta_i)cos(\varphi_i), \sin(\varphi_i)]^T$ is the vector from the UAV to the target at the ith measurement.

The cost function based on the WLS estimator is constructed to find the closed-form solution in (10) [26], which is expressed as

$$f = (\boldsymbol{F}\boldsymbol{x} - \boldsymbol{h})^T\boldsymbol{W}(\boldsymbol{F}\boldsymbol{x} - \boldsymbol{h}). \tag{13}$$

In WLS estimator, the solution of (10) is the $\boldsymbol{x}$ that minimizes the cost function f. However, this solution is biased and the reason is analysed in the next. Let $\boldsymbol{A} = [\boldsymbol{F}, -\boldsymbol{h}]$, $\boldsymbol{y} = [\boldsymbol{x}, 1]^T$ and $\boldsymbol{\Psi} = \boldsymbol{A}^T\boldsymbol{W}\boldsymbol{A} - \boldsymbol{A_0}^T\boldsymbol{W}\boldsymbol{A_0} = \boldsymbol{A}^T\boldsymbol{W}\boldsymbol{A} - \boldsymbol{\Psi_0}$, where $\boldsymbol{A}_0$ is the matrix $\boldsymbol{A}$ with the measurements replaced by the real ones and $\boldsymbol{\Psi_0} = \boldsymbol{A_0}^T\boldsymbol{W}\boldsymbol{A_0}$. Rewrite f as

$$f = \boldsymbol{y}^T\boldsymbol{A}^T\boldsymbol{W}\boldsymbol{A}\boldsymbol{y} = \boldsymbol{y}^T\boldsymbol{\Psi_0}\boldsymbol{y} + \boldsymbol{y}^T\boldsymbol{\Psi}\boldsymbol{y}. \tag{14}$$

The expectation of (14) is

$$E\{f\} = \boldsymbol{y}^T\boldsymbol{\Psi_0}\boldsymbol{y} + \boldsymbol{y}^T E\{\boldsymbol{\Psi}\}\boldsymbol{y}, \tag{15}$$

If $E\{\boldsymbol{\Psi}\}$ in (15) is equal to zero, it is obvious that the minimum of $E\{f\}$ is determined by the first term and it can reach the minimum 0 at the ideal solution $\boldsymbol{y} = [\boldsymbol{x}, 1]^T$. However, in practice, $E\{\boldsymbol{\Psi}\}$ is not equal to zero, which is the reason of the biased solution. In order to reduce the bias, the idea is to minimize f subject to $\boldsymbol{y}^T E\{\boldsymbol{\Psi}\}\boldsymbol{y}$ equal to a constant c, which means that the minimum of $E\{f\}$ is determined by the first term in (15) like $E\{\boldsymbol{\Psi}\} = 0$. This ideal is described by a mathematical formula as follows,

$$\begin{aligned} f_{min} &= \boldsymbol{y}^T \boldsymbol{A}^T \boldsymbol{W} \boldsymbol{A} \boldsymbol{y} \\ &\text{subject to } \boldsymbol{y}^T E\{\boldsymbol{\Psi}\}\boldsymbol{y} = c, \end{aligned} \tag{16}$$

It is obvious that the minimum of the cost function f in (16) is the constrained weighted least-squares problem. The constrained optimization problem will be solved by the Lagrange multiplier (LM) method. The auxiliary function constructed by the LM method is given as

$$\boldsymbol{y}^T \boldsymbol{A}^T \boldsymbol{W} \boldsymbol{A} \boldsymbol{y} + \chi(c - \boldsymbol{y}^T E\{\boldsymbol{\Psi}\}\boldsymbol{y}), \tag{17}$$

where χ is the Lagrange multiplier. Taking the partial derivative with respect to $\boldsymbol{y}$ and setting it equal to zero,

$$\boldsymbol{A}^T \boldsymbol{W} \boldsymbol{A} \boldsymbol{y} = \chi E\{\boldsymbol{\Psi}\}\boldsymbol{y}. \tag{18}$$

According to (18), the solution of $\boldsymbol{y}$ should be the generalized eigenvector of $[\boldsymbol{A}^T \boldsymbol{W} \boldsymbol{A}, E\{\boldsymbol{\Psi}\}]$. However, the generalized eigenvectors are often not unique. By multiplying $\boldsymbol{y}^T$ in (18), the equation can be rewritten as

$$\boldsymbol{y}^T \boldsymbol{A}^T \boldsymbol{W} \boldsymbol{A} \boldsymbol{y} = \chi \boldsymbol{y}^T E\{\boldsymbol{\Psi}\}\boldsymbol{y} = \chi c. \tag{19}$$

It is obvious that the χc is the cost function to be minimized. Hence the solution of $\boldsymbol{y}$ is the eigenvector $\boldsymbol{\xi}$ corresponding to the smallest generalized eigenvalue of $[\boldsymbol{A}^T \boldsymbol{W} \boldsymbol{A}, E\{\boldsymbol{\Psi}\}]$ [14]. The closed-form solution of the proposed IBRPLE can be given as

$$\boldsymbol{x} = \frac{\boldsymbol{\xi}(1:6, 1)}{\boldsymbol{\xi}(7, 1)}. \tag{20}$$

B. THE IMPROVED WEIGHTING MATRIX

The weighting matrix is inaccurate in (12) due to the neglect of the azimuth angle error in ν_i, which will be recalculated in the subsection. Rewrite (9) as

$$\begin{aligned} \mu_i &= \hat{\boldsymbol{b}}_i^T \boldsymbol{p}_i - \hat{\boldsymbol{b}}_i^T \hat{\boldsymbol{s}}_i = \hat{\boldsymbol{b}}_i^T \boldsymbol{p}_i - \hat{\boldsymbol{b}}_i^T (\boldsymbol{s}_i + \Delta \boldsymbol{s}_i) \\ &= \hat{\boldsymbol{b}}_i^T \boldsymbol{r}_i - \hat{\boldsymbol{b}}_i^T \Delta \boldsymbol{s}_i \\ &= \begin{bmatrix} \sin(\hat{\theta}_i) \\ -\cos(\hat{\theta}_i) \\ 0 \end{bmatrix}^T \left(d_i \begin{bmatrix} \cos(\theta_i)\cos(\varphi_i) \\ \sin(\theta_i)\cos(\varphi_i) \\ \sin(\varphi_i) \end{bmatrix} - \begin{bmatrix} \Delta x_i \\ \Delta y_i \\ \Delta z_i \end{bmatrix} \right) \\ &= d_i \cos(\varphi_i)\sin(n_i) - [\Delta x_i \sin(\hat{\theta}_i) - \Delta y_i \cos(\hat{\theta}_i)], \end{aligned} \tag{21}$$

$$\begin{aligned} \nu_i &= \hat{\boldsymbol{c}}_i^T \boldsymbol{p}_i - \hat{\boldsymbol{c}}_i^T \hat{\boldsymbol{s}}_i = \hat{\boldsymbol{c}}_i^T \boldsymbol{p}_i - \hat{\boldsymbol{c}}_i^T (\boldsymbol{s}_i + \Delta \boldsymbol{s}_i) \\ &= \hat{\boldsymbol{c}}_i^T \boldsymbol{r}_i - \hat{\boldsymbol{c}}_i^T \Delta \boldsymbol{s}_i \\ &= \begin{bmatrix} \cos(\hat{\theta}_i)\sin(\hat{\varphi}_i) \\ \sin(\hat{\theta}_i)\sin(\hat{\varphi}_i) \\ -\cos(\hat{\varphi}_i) \end{bmatrix}^T \left(d_i \begin{bmatrix} \cos(\theta_i)\cos(\varphi_i) \\ \sin(\theta_i)\cos(\varphi_i) \\ \sin(\varphi_i) \end{bmatrix} - \begin{bmatrix} \Delta x_i \\ \Delta y_i \\ \Delta z_i \end{bmatrix} \right) \\ &= d_i[\cos(n_i)\cos(\varphi_i)\sin(\hat{\varphi}_i) - \cos(\hat{\varphi}_i)\sin(\varphi_i)] \\ &\quad - [\Delta x_i \cos(\hat{\theta}_i)\sin(\hat{\varphi}_i) + \Delta y_i \sin(\hat{\theta}_i)\sin(\hat{\varphi}_i) \\ &\quad - \Delta z_i \cos(\hat{\varphi}_i)], \end{aligned} \tag{22}$$

According to the definition, the inverse of the weighting matrix is the covariance matrix of the error vector, which is rewritten as

$$\boldsymbol{W}^{-1} = E\{\boldsymbol{\eta}\boldsymbol{\eta}^T\} = E\left\{ \begin{bmatrix} \mu_0 \\ \mu_1 \\ \vdots \\ \mu_{N-1} \\ \nu_0 \\ \nu_1 \\ \vdots \\ \nu_{N-1} \end{bmatrix} \begin{bmatrix} \mu_0 \\ \mu_1 \\ \vdots \\ \mu_{N-1} \\ \nu_0 \\ \nu_1 \\ \vdots \\ \nu_{N-1} \end{bmatrix}^T \right\} \tag{23}$$

In order to calculate the weighting matrix $\boldsymbol{W}$ in (23), the expectations of $\mu_k \mu_j$, $\nu_k \nu_j$, and $\mu_k \nu_j$ for the arbitrary k, j should be calculated as a premise. Because two measurements for $k \neq j$ are independent, here we have [24]

$$\begin{aligned} &E\{\mu_k \mu_j\} = E\{\mu_k \nu_j\} = E\{\nu_k \nu_j\} = 0 \\ &\text{for} \quad k, j = 0, 1, \ldots, N-1 \quad \text{and} \quad k \neq j \end{aligned} \tag{24}$$

For $k = j = i$, the expectations of $\mu_i \nu_i$, $\mu_i \mu_i$ and $\nu_i \nu_i$ are calculated in appendix A, which are respectively given as

$$\begin{aligned} E\{\mu_i \nu_i\} &= 0, \\ E\{\mu_i \mu_i\} &= l_i^2 \sigma_i^2 + \sigma_{si}^2, \\ E\{\nu_i \nu_i\} &= \rho_i^2 (d_i^2 - \sigma_i^2 l_i^2) + \sigma_{si}^2. \end{aligned} \tag{25}$$

With these expectations, the inverse of the improved weighting matrix $\boldsymbol{W}$ can be written as

$$\boldsymbol{W}^{-1} = diag\left(\begin{bmatrix} l_0^2 \sigma_0^2 + \sigma_{s0}^2 \\ l_1^2 \sigma_1^2 + \sigma_{s1}^2 \\ \vdots \\ l_{N-1}^2 \sigma_{N-1}^2 + \sigma_{s(N-1)}^2 \\ \rho_0^2 (d_0^2 - \sigma_0^2 l_0^2) + \sigma_{s0}^2 \\ \rho_1^2 (d_1^2 - \sigma_1^2 l_1^2) + \sigma_{s1}^2 \\ \vdots \\ \rho_{N-1}^2 (d_{N-1}^2 - \sigma_{N-1}^2 l_{N-1}^2) + \sigma_{s(N-1)}^2 \end{bmatrix} \right). \tag{26}$$

C. THE CALCULATION OF THE BIASED TERM WITH HIGHER PRECISION

In (16), $E\{\boldsymbol{\Psi}\}$ should be calculated as a premise to find the solution of the constrained weighted least-squares problem. However, the calculation of $E\{\boldsymbol{\Psi}\}$ is not easy due to the nonlinear relation between the AOA errors and the coefficients of pseudo linear equations. In this subsection, the method is developed to calculate $E\{\boldsymbol{\Psi}\}$ with higher precision. The ideal of calculating $E\{\boldsymbol{\Psi}\}$ is to calculate $E\{\boldsymbol{A}^T \boldsymbol{W} \boldsymbol{A}\}$ in the first step. Subsequently, $E\{\boldsymbol{\Psi}\}$ can be obtained by $E\{\boldsymbol{A}^T \boldsymbol{W} \boldsymbol{A}\} - \boldsymbol{A}_0^T \boldsymbol{W} \boldsymbol{A}_0$.

The expectation of $\boldsymbol{A}^T\boldsymbol{W}\boldsymbol{A}$ can be calculated as (See appendix B in details),

$$\begin{aligned}\boldsymbol{\Gamma} &= E\{\boldsymbol{A}^T\boldsymbol{W}\boldsymbol{A}\}\\ &= E\{[\boldsymbol{F}-\boldsymbol{h}]^T\boldsymbol{W}[\boldsymbol{F}-\boldsymbol{h}]\}\\ &= E\left\{\begin{bmatrix}\boldsymbol{F}^T\boldsymbol{W}\boldsymbol{F} & -\boldsymbol{F}^T\boldsymbol{W}\boldsymbol{h}\\ -(\boldsymbol{F}^T\boldsymbol{W}\boldsymbol{h})^T & \boldsymbol{h}^T\boldsymbol{W}\boldsymbol{h}\end{bmatrix}\right\}\\ &= E\left\{\begin{bmatrix}\boldsymbol{Z}_1 & -\boldsymbol{Z}_2\\ -\boldsymbol{Z}_2^T & \boldsymbol{Z}_3\end{bmatrix}\right\}\\ &= \begin{bmatrix}E\{\boldsymbol{Z}_1\} & -E\{\boldsymbol{Z}_2\}\\ -E\{\boldsymbol{Z}_2^T\} & E\{\boldsymbol{Z}_3\}\end{bmatrix}\end{aligned}\tag{27}$$

where

$$\begin{cases}E\{\boldsymbol{Z}_1\} = \boldsymbol{Z}_1^0 + \Delta\boldsymbol{Z}_1,\\ E\{\boldsymbol{Z}_2\} = \boldsymbol{Z}_2^0 + \Delta\boldsymbol{Z}_2,\\ E\{\boldsymbol{Z}_3\} = \boldsymbol{Z}_3^0 + \Delta\boldsymbol{Z}_3,\end{cases}\tag{28}$$

where $\boldsymbol{Z}_i^0$ is the real value and $\Delta\boldsymbol{Z}_i$ is the bias term caused by the AOA errors and the position errors of the UAV. Consequently, $\boldsymbol{A}_0^T\boldsymbol{W}\boldsymbol{A}_0$ can be expressed by $\boldsymbol{Z}_i^0$ as

$$\boldsymbol{A}_0^T\boldsymbol{W}\boldsymbol{A}_0 = \begin{bmatrix}\boldsymbol{Z}_1^0 & -\boldsymbol{Z}_2^0\\ -\boldsymbol{Z}_2^{0T} & \boldsymbol{Z}_3^0\end{bmatrix}\tag{29}$$

It is obvious that $E\{\boldsymbol{\Psi}\}$ can be given as

$$E\{\boldsymbol{\Psi}\} = \begin{bmatrix}\Delta\boldsymbol{Z}_1 & -\Delta\boldsymbol{Z}_2\\ -\Delta\boldsymbol{Z}_2^T & \Delta\boldsymbol{Z}_3\end{bmatrix}\tag{30}$$

According to appendix B, the bias terms of $\boldsymbol{Z}_1$, $\boldsymbol{Z}_2$ and $\boldsymbol{Z}_3$ are obtained as

$$\begin{cases}\Delta\boldsymbol{Z}_1 = \sum_{i=0}^{N-1} w_{1i}\boldsymbol{M}_i^T\Delta\boldsymbol{J}_{1i}\boldsymbol{M}_i + w_{2i}\boldsymbol{M}_i^T\Delta\boldsymbol{J}_{2i}\boldsymbol{M}_i,\\ \Delta\boldsymbol{Z}_2 = \sum_{i=0}^{N-1} w_{1i}\boldsymbol{M}_i^T\Delta\boldsymbol{J}_{1i}\boldsymbol{s}_i + w_{2i}\boldsymbol{M}_i^T\Delta\boldsymbol{J}_{2i}\boldsymbol{s}_i,\\ \Delta\boldsymbol{Z}_3 = \sum_{i=0}^{N-1} w_{1i}\boldsymbol{s}_i^T\Delta\boldsymbol{J}_{1i}\boldsymbol{s}_i + w_{2i}\boldsymbol{s}_i^T\Delta\boldsymbol{J}_{2i}\boldsymbol{s}_i\\ +\sum_{i=0}^{N-1} w_{1i}\sigma_{si}^2 + w_{2i}\sigma_{si}^2,\end{cases}\tag{31}$$

where $w_{2i} = 1/(\rho_i^2(d_i^2 - \sigma_i^2 l_i^2) + \sigma_{si}^2)$ are the diagonal elements of the improved weighting matrix $\boldsymbol{W}$, $\Delta\boldsymbol{J}_{1i}$ and $\Delta\boldsymbol{J}_{2i}$ can be written as

$$\Delta\boldsymbol{J}_{1i} = \sigma_i^2\begin{bmatrix}\cos(2\theta_i) & \sin(2\theta_i) & 0\\ \sin(2\theta_i) & -\cos(2\theta_i) & 0\\ 0 & 0 & 0\end{bmatrix},\tag{32}$$

$$\Delta\boldsymbol{J}_{2i} = \sigma_i^2\begin{bmatrix}g_1 & g_2 & g_3\\ g_2 & g_4 & g_5\\ g_3 & g_5 & g_6\end{bmatrix},\tag{33}$$

where

$$\begin{aligned}g_1 &= -\sigma_i^2\cos(2\theta_i)\sin^2(\varphi_i) + \rho_i^2\cos^2(\theta_i)\cos(2\varphi_i),\\ g_2 &= -\sigma_i^2\sin(2\theta_i)\sin^2(\varphi_i) + \frac{\rho_i^2}{2}\sin(2\theta_i)\cos(2\varphi_i),\\ g_3 &= \frac{\sigma_i^2}{4}\cos(\theta_i)\sin(2\varphi_i) + \rho_i^2\cos(\theta_i)\sin(2\varphi_i),\\ g_4 &= \sigma_i^2\cos(2\theta_i)\sin^2(\varphi_i) + \rho_i^2\sin^2(\theta_i)\cos(2\varphi_i),\\ g_5 &= \frac{\sigma_i^2}{4}\sin(\theta_i)\sin(2\varphi_i) + \rho_i^2\sin(\theta_i)\sin(2\varphi_i),\\ g_6 &= \rho_i^2\cos(2\varphi_i).\end{aligned}\tag{34}$$

IV. IMPROVING THE ACCURACY OF LOCALIZATION BY THE UAV PATH PLANNING

In this section, the path planning algorithm with the position errors of the UAV is discussed to further improve the localization accuracy. In [32], the localization accuracy is evaluated by the 1σ error ellipse area $A_{1\sigma}$ (39.4% confidence region), which shows that the result of the maximum likelihood estimation falls in the region of the area $A_{1\sigma}$ with a probability of 39.4%. Therefore, the localization accuracy is high when the area $A_{1\sigma}$ is small. $A_{1\sigma}$ has been demonstrated in [32] to have the form $A_{1\sigma} = \pi/(\sqrt{\det(\boldsymbol{\Omega}(\boldsymbol{x}))})$, where $\boldsymbol{\Omega}(\boldsymbol{x})$ is the FIM of $\boldsymbol{x}$. It is obvious that between the minimizing the area $A_{1\sigma}$ and the maximizing the determinant $\det(\boldsymbol{\Omega}(\boldsymbol{x}))$ of FIM to obtain the highest localization accuracy are equivalent. Therefore, the determinant maximization criterion of FIM will be used to design the path of the UAV. The FIM is defined in [30] as

$$\boldsymbol{\Omega}(z) = E\left\{\left[\frac{\partial\ln f(\boldsymbol{m})}{\partial z^T}\right]^T\left[\frac{\partial\ln f(\boldsymbol{m})}{\partial z^T}\right]\right\},\tag{35}$$

where $z = [\boldsymbol{p}_0^T, \boldsymbol{v}^T, \boldsymbol{s}^T]^T$, $\boldsymbol{m} = [\hat{\boldsymbol{\theta}}^T, \hat{\boldsymbol{\varphi}}^T, \hat{\boldsymbol{s}}^T]^T$, $f(\boldsymbol{m})$ is the probability density function (PDF) of the $\boldsymbol{m}$ measurements [24]. Because the errors of the AOA measurements and the UAV positions submit the independent Gaussian distribution, $f(\boldsymbol{m})$ can be expressed as the product between the PDF of the AOA errors and the PDF of the UAV position errors,

$$\begin{aligned}f(\boldsymbol{m}) &= \frac{1}{(2\pi)^{3N/2}\det(\boldsymbol{Q}_m)}\\ &\quad\times\exp\{-\frac{1}{2}(\boldsymbol{m}-\boldsymbol{m}_0)^T\boldsymbol{Q}_m^{-1}(\boldsymbol{m}-\boldsymbol{m}_0)\}\\ &= \frac{1}{(2\pi)^N\det(\boldsymbol{Q}_a)}\exp\{-\frac{1}{2}(\boldsymbol{a}-\boldsymbol{a}_0)^T\boldsymbol{Q}_a^{-1}(\boldsymbol{a}-\boldsymbol{a}_0)\}\\ &\quad\times\frac{1}{(2\pi)^{N/2}\det(\boldsymbol{Q}_s)}\exp\{-\frac{1}{2}(\hat{\boldsymbol{s}}-\boldsymbol{s})^T\boldsymbol{Q}_s^{-1}(\hat{\boldsymbol{s}}-\boldsymbol{s})\},\end{aligned}\tag{36}$$

where $\boldsymbol{m}_0 = [\boldsymbol{\theta}^T, \boldsymbol{\varphi}^T, \boldsymbol{s}^T]^T$, $\boldsymbol{a} = [\hat{\boldsymbol{\theta}}^T, \hat{\boldsymbol{\varphi}}^T]^T$ is the AOA measurements, $\boldsymbol{a}_0 = [\boldsymbol{\theta}^T, \boldsymbol{\varphi}^T]^T$ is the real AOA,

$$\begin{aligned}\boldsymbol{Q}_m &= \begin{bmatrix}\boldsymbol{Q}_n & & \\ & \boldsymbol{Q}_\omega & \\ & & \boldsymbol{Q}_s\end{bmatrix},\\ \boldsymbol{Q}_a &= \begin{bmatrix}\boldsymbol{Q}_n & \\ & \boldsymbol{Q}_\omega\end{bmatrix}.\end{aligned}\tag{37}$$

In order to calculate FIM, the logarithm of $f(\boldsymbol{m})$ is required to be calculated in advance, which is obtained from (36) as

$$\ln f(\boldsymbol{m}) = C - \frac{1}{2}(\boldsymbol{a}-\boldsymbol{a}_0)^T \boldsymbol{Q}_a^{-1}(\boldsymbol{a}-\boldsymbol{a}_0) - \frac{1}{2}(\hat{\boldsymbol{s}}-\boldsymbol{s})^T \boldsymbol{Q}_s^{-1}(\hat{\boldsymbol{s}}-\boldsymbol{s}), \quad (38)$$

where C is constant. Putting (38) into (35), the FIM of z is given as

$$\begin{aligned}\boldsymbol{\Omega}(z) &= E\{\left[(\boldsymbol{a}-\boldsymbol{a}_0)^T \boldsymbol{Q}_a^{-1}\frac{\partial \boldsymbol{a}_0}{\partial z^T} + (\hat{\boldsymbol{s}}-\boldsymbol{s})^T \boldsymbol{Q}_s^{-1}\frac{\partial \boldsymbol{s}}{\partial z^T}\right]^T \\ &\quad \times \left[(\boldsymbol{a}-\boldsymbol{a}_0)^T \boldsymbol{Q}_a^{-1}\frac{\partial \boldsymbol{a}_0}{\partial z^T} + (\hat{\boldsymbol{s}}-\boldsymbol{s})^T \boldsymbol{Q}_s^{-1}\frac{\partial \boldsymbol{s}}{\partial z^T}\right]\} \\ &= \left[\frac{\partial \boldsymbol{a}_0}{\partial z^T}\right]^T \boldsymbol{Q}_a^{-1}\frac{\partial \boldsymbol{a}_0}{\partial z^T} + \left[\frac{\partial \boldsymbol{s}}{\partial z^T}\right]^T \boldsymbol{Q}_s^{-1}\frac{\partial \boldsymbol{s}}{\partial z^T}. \quad (39)\end{aligned}$$

Details are provided in Appendix C. Let $\boldsymbol{G_x} = \frac{\partial \boldsymbol{a}_0}{\partial \boldsymbol{x}^T}$ and $\boldsymbol{G_s} = \frac{\partial \boldsymbol{a}_0}{\partial \boldsymbol{s}^T}$, here we have $\frac{\partial \boldsymbol{a}_0}{\partial z^T} = [\boldsymbol{G_x}, \boldsymbol{G_s}]$. $\frac{\partial \boldsymbol{s}}{\partial z^T}$ can be rewritten as $\left[\frac{\partial \boldsymbol{s}}{\partial \boldsymbol{x}^T}, \frac{\partial \boldsymbol{s}}{\partial \boldsymbol{s}^T}\right] = [\boldsymbol{0}_{3N\times 6}, \boldsymbol{I}_{3N}]$ due to $\boldsymbol{s}$ without the variable $\boldsymbol{x}$. The FIM of z can be simplified as

$$\boldsymbol{\Omega}(z) = \begin{bmatrix} \boldsymbol{Y}_1 & \boldsymbol{Y}_2 \\ \boldsymbol{Y}_2^T & \boldsymbol{Y}_3 \end{bmatrix}, \quad (40)$$

where $\boldsymbol{Y}_1 = \boldsymbol{G_x}^T \boldsymbol{Q}_a^{-1}\boldsymbol{G_x}$, $\boldsymbol{Y}_2 = \boldsymbol{G_x}^T \boldsymbol{Q}_a^{-1}\boldsymbol{G_s}$ and $\boldsymbol{Y}_3 = \boldsymbol{G_s}^T \boldsymbol{Q}_a^{-1}\boldsymbol{G_s} + \boldsymbol{Q}_s^{-1}$. Because the CRLB is equal to the inverse of the FIM, the CRLB of $\boldsymbol{x}$ and $\boldsymbol{s}$ can be given from (40) as

$$\begin{aligned} CRLB(\boldsymbol{x}) &= (\boldsymbol{Y}_1 - \boldsymbol{Y}_2\boldsymbol{Y}_3^{-1}\boldsymbol{Y}_2^T)^{-1}, \\ CRLB(\boldsymbol{s}) &= (\boldsymbol{Y}_3 - \boldsymbol{Y}_2^T\boldsymbol{Y}_1^{-1}\boldsymbol{Y}_2)^{-1}. \quad (41)\end{aligned}$$

According to the mathematical expression in (41), $CRLB(\boldsymbol{x})$ can be expressed by $CRLB(\boldsymbol{s})$ [37] as

$$CRLB(\boldsymbol{x}) = \boldsymbol{Y}_1^{-1} + \boldsymbol{Y}_1^{-1}\boldsymbol{Y}_2 CRLB(s)\boldsymbol{Y}_2^T\boldsymbol{Y}_1^{-1}. \quad (42)$$

Eq. (42) shows that the CRLB of $\boldsymbol{x}$ is mainly determined by the AOA errors and the position errors of the UAV. The first term indicates the uncertainty of the localization caused by the AOA errors. The second term indicates the influence of the position errors of the UAV on the localziation performance. If the position of the UAV is accurate, i.e., $CRLB(\boldsymbol{s}) = \boldsymbol{0}$, it is obvious that the CRLB of $\boldsymbol{x}$ is only related to the AOA errors. However, the position of the UAV is usually inaccurate, which will result in some increase in $CRLB(\boldsymbol{x})$. This is the reason why the position errors of the UAV lead to the degradation of the localization accuracy. The past path planning only considered that how to reduce the impact of the AOA errors on localization accuracy. However, it is necessary to consider how to reduce the impact of the UAV position error on the localization accuracy in path planning, because it will also lead to the degradation of localization performance.

The determinant maximization criterion of FIM is used in path planning, so the FIM of $\boldsymbol{x}$ need to be calculated and is obtained by (42) as

$$\boldsymbol{\Omega}(\boldsymbol{x}) = \boldsymbol{Y}_1 - \boldsymbol{Y}_2\boldsymbol{Y}_3^{-1}\boldsymbol{Y}_2^T \quad (43)$$

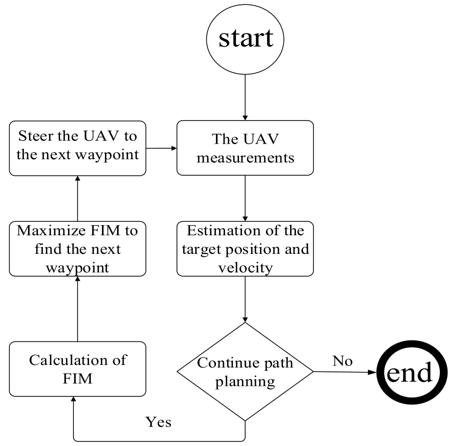

FIGURE 2. The flowchart of the UAV path planning and the target localization based on maximizing the determinant of FIM.

Then, how to plan the path of UAV will be discussed. According to (35), the localization performance is improved by maximizing the determinant of FIM. Obviously we can solve such a problem by the gradient rise method. However, it is difficult to calculate the partial derivative of the determinant $\det(\boldsymbol{\Omega}(\boldsymbol{x}))$ with respect to $\boldsymbol{s}_i$. Therefore, we will take an approximate approach to find the optimal path. The partial derivative of $\boldsymbol{\Omega}(\boldsymbol{x})$ with respect to x axis is derived as an example. Let ϵ be a value close to zero. Let $\boldsymbol{s}_{i+1} = \boldsymbol{s}_i + [\epsilon, 0, 0]^T$. The partial derivative G_x can be calculated as the follow

$$\begin{aligned} G_x &= \frac{\partial \det(\boldsymbol{\Omega}(\boldsymbol{x}))}{\partial x} \\ &\approx \frac{\det(\boldsymbol{\Omega}(\boldsymbol{x}, \boldsymbol{s}^{i+1})) - \det(\boldsymbol{\Omega}(\boldsymbol{x}, \boldsymbol{s}_i))}{\epsilon} \quad (44)\end{aligned}$$

G_y and G_z can be calculated by the same method. The normalized gradient direction of the determinant of the $\boldsymbol{\Omega}(\boldsymbol{x})$ is $\boldsymbol{G} = [G_x, G_y, G_z]^T / \|[G_x, G_y, G_z]^T\|$. Assume that the speed of the UAV is a constant v_u. The next position of UAV is calculated as follows

$$\boldsymbol{s}_{i+1} = \boldsymbol{s}_i + \boldsymbol{G}v_u T \quad (45)$$

In order to clearly understand these methods, the detailed steps of the path planning and the target localization are shown in Fig.2. It is obvious that the UAV should randomly fly several waypoints to obtain AOA measurements. the initial estimate of the target position can be calculated by the IBRPLE method. Subsequently,the initial estimate is used in path planning. The path planning and target localization methods are alternately executed until the constraint (the range constraint, the time constraint, and so on) is reached.

V. SIMULATION RESULTS

In this section, the localization performance comparison between the proposed IBRPLE method and various methods (IPLE and IIV in [24], BRPLE in [26]) is given in Fig.3-4 to show the higher accuracy of localization achieved by the

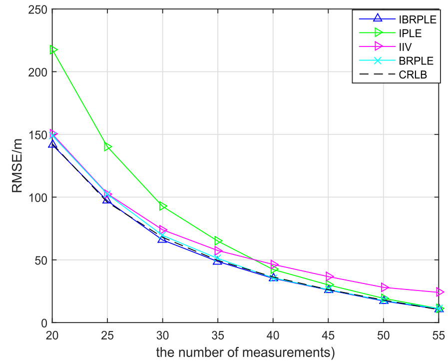

FIGURE 3. The localization performance comparison between different algorithms versus the number of measurements.

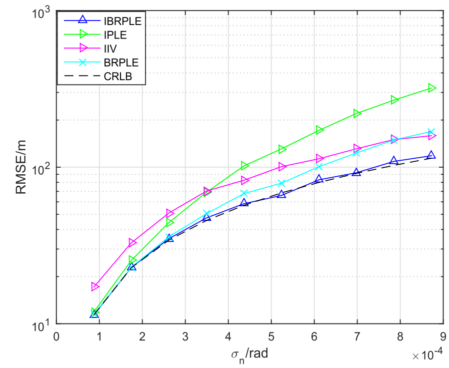

FIGURE 4. The localization performance comparison between different algorithms versus the reference standard deviation σ_n.

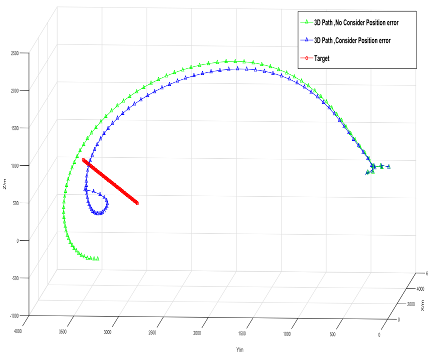

FIGURE 5. Paths of the UAV in two different path planning methods.

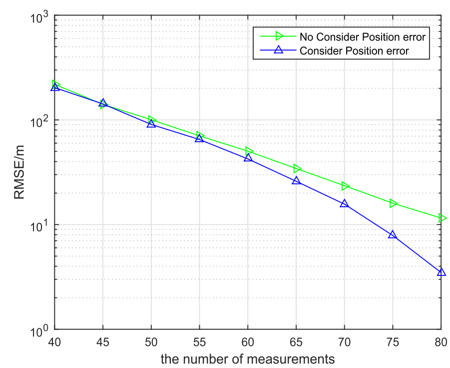

FIGURE 6. RMSE of two paths in two different path planning methods.

IBRPLE method. The path of the UAV is simulated in Fig.5 to show the importance of considering the position errors of UAV in path planning.

In Fig.3-4, we assume that the target is fixed, the position of target is $\boldsymbol{p}_0 = [4000, 3000, 100]m$, the initial position of the UAV is $\boldsymbol{s} = [300, 500, 700, 900, 1100, 1300, 1500; 0, 100, 100, 200, 200, 300, 300; 1000, 1000, 950, 950, 900, 800, 800]^T m$, the power loss exponent is $\lambda = 1.2$, the reference standard deviation of azimuth angle is $\sigma_n = (0.005 \times \pi/180)rad$, the reference standard deviation of elevation angle is $\sigma_\omega = (0.005 \times \pi/180)rad$, the standard deviation of position of the UAV is $\sigma_{S0} = \sigma_{S1} = \cdots = \sigma_{S(N-1)} = 0.2m$, the interval of measurement is $T = 5s$.

In Fig.3, the performance of localization for different localization methods is simulated with the change of the number N of measurements. All the performance curves become smaller as the number of measurements increases, which means that the performance of localization can be improved by the large N. As shown in Fig.3, when the number of measurements is relatively small, the proposed IBRPLE method can achieve higher accuracy of localization than the other methods. The reason behind this observation is that the bias is effectively reduced by using IBRPLE method. On the other hand, for large N, the methods except IIV method can achieve almost same RMSE. This is because the weighting matrix is not considered in the IIV method which causes the equations with the different error to have the same weight, its performance of localization is mainly determined by the equation with a large error. The localization accuracy of the proposed IBRPLE method is always close to that of CRLB, which shows that the IBRPLE method is feasible and has a high accuracy for target localization.

Fig.4 shows the performance of localization for different localization methods versus the variance of the measurement angle. We assume that the number of measurements is $N = 55$, and the reference variances of the azimuth angle and elevation angle at unit range are equal. It can be seen from the Fig.4 that the errors of localization will increase with the increase of the standard deviation of the angle measurement. At the small σ_n, the localization performance of most algorithms are almost identical and are close to CRLB, which shows that all algorithms have good performance of localization when the accuracy of AOA measurement is high. However, only the localization performance of the IBRPLE algorithm is still close to CRLB when σ_n is large. The proposed IBRPLE has better robustness to the impact of angular errors compared to several algorithms. The performance degradation of other algorithms is mainly caused by the bias of closed-form solutions.

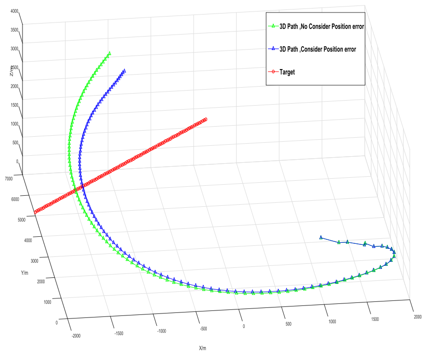

FIGURE 7. Paths of the UAV in two different path planning methods.

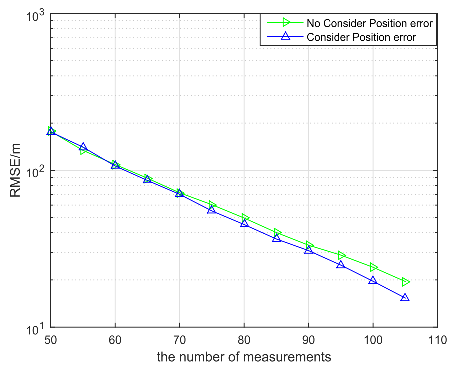

FIGURE 8. RMSE of two paths in two different path planning methods.

Fig.5 and Fig.6 illustrate the paths of the UAV for different path planning schemes and corresponding localization performances, respectively. The simulation parameters are set as follows: the initial position of target is $\boldsymbol{p}_0 = [4000, 3000, 100]m$, the speed of target is $\boldsymbol{v} = [1, 0.8, 0.6]^T m/s$. The initial position of the UAV is $\boldsymbol{s} = [300, 500, 700, 900, 1100, 1300, 1500; 0, 100, 100, 200, 200, 300, 300; 1000, 1000, 950, 950, 900, 800, 800]^T m$, the speed of UAV is $\boldsymbol{v}_u = 20m/s$, $\sigma_n = \sigma_\omega = (0.005 \times \pi/180)rad$, the standard deviation of position of the UAV is $\sigma_{s0} = \sigma_{s1}, \cdots, \sigma_{s(N-1)} = 0.8m$, and the interval of measurement is $T = 5s$.

Two paths of the UAV corresponding to different path planing schemes are shown in Fig.6, one of which considers the position errors of the UAV in our proposed path planing scheme, and the other ignores the position errors. It is obvious that the two paths are different. Corresponding error curves of localization are shown in the Fig.6. For the small N, the localization performance of for two path planing schemes is almost the same since the initial position of two paths are approximately the same. For the large N, The higher localization accuracy for the path planing which considers position errors of the UAV can be achieved, as shown in Fig. 5. The reason behind this observation is that the adverse impact of position errors of the UAV on localization performance can be reduced accordingly if the position errors are considered in path planning.

In order to further illustrate the advantages of path planning proposed in this paper, the path of the UAV is once again simulated with different simulation parameters in Fig.7 and Fig.8. The initial position of target is $\boldsymbol{p}_0 = [4000, 3000, 100]m$, the speed of target is $\boldsymbol{v} = [2, 1.6, 1.2]^T m/s$. the initial position of the UAV is $\boldsymbol{s} = [1000, 1200, 1300, 1500, 1500, 1600, 1700; 500, 4000, 400, 400, 300, 300, 300; 1500, 1400, 1400, 1300, 1400, 1300, 1300]^T m$, the speed of UAV is $v_u = 20m/s$, $\sigma_n = \sigma_\omega = (0.005 \times \pi/180)rad$, the standard deviation of position of the UAV is $\sigma_{s0} = \sigma_{s1} = \cdots = \sigma_{s(N-1)} = 1.5m$, and the interval of measurement is $T = 5s$. The paths of the UAV for different path planning schemes and corresponding localization performances are shown in Fig.6 and Fig.7, respectively. The path planning scheme proposed in this paper that considers the position error of the UAV can achieve the better localization performance.

VI. CONCLUSION

In this paper, the localization performance for the bearing-only target localization based on the UAV is improved from two aspects. On the one hand, in order to reduce the bias, the weighting matrix is recalculated more accurately and the improved bias reduction pseudo-linear estimator (IBRPLE) is proposed which achieves better localization performance verified by simulation. On the other hand, a path planning algorithm considering the position errors of the UAV is proposed to reduce the adverse impact of position errors of the UAV on localization performance. The simulation shows that the path planning scheme considering the position errors of the UAV can achieve the better localization performance.

APPENDIX A

Let us calculate the expectation of the product of μ_i and ν_i

$$
\begin{aligned}
&E\{\mu_i \nu_i\} \\
&\quad = E\{\{d_i \cos(\varphi_i) \sin(n_i) \\
&\qquad - [\Delta x \sin(\hat{\theta}_i) - \Delta y \cos(\hat{\theta}_i)]\} \\
&\qquad \cdot \{d_i[\cos(n_i) \cos(\varphi_i) \sin(\hat{\varphi}_i) - \cos(\hat{\varphi}_i) \sin(\varphi_i)] \\
&\qquad - [\Delta x \cos(\hat{\theta}_i) \sin(\hat{\varphi}_i) + \Delta y \sin(\hat{\theta}_i) \sin(\hat{\varphi}_i) \\
&\qquad - \Delta z \cos(\hat{\varphi}_i)]\}\} \\
&\quad = \frac{1}{2} d_i^2 \cos(\varphi_i) E\{sin(2n_i)\} E\{\sin(2\hat{\varphi}_i)\} \\
&\qquad - E\{\Delta x_i^2\} E\{\sin(\hat{\theta}_i) \cos(\hat{\theta}_i) \sin(\hat{\varphi}_i)\} \\
&\qquad + E\{\Delta y_i^2\} E\{\sin(\hat{\theta}_i) \cos(\hat{\theta}_i) \sin(\hat{\varphi}_i)\} \\
&\quad = d_i^2 \cos(\varphi_i) E\{n_i\} \\
&\qquad + E\{\sin(\hat{\theta}_i) \cos(\hat{\theta}_i) \sin(\hat{\varphi}_i)\} \\
&\qquad \cdot (E\{\Delta y_i^2\} - E\{\Delta x_i^2\}) \\
&\quad = 0
\end{aligned} \tag{46}
$$

$$
\begin{aligned}
&E\{\mu_i\mu_i\}\\
&\quad = E\{\{d_i\cos(\varphi_i)\sin(n_i)\\
&\qquad -[\Delta x\sin(\hat{\theta}_i)-\Delta y\cos(\hat{\theta}_i)]\}^2\}\\
&\quad = d_i^2\cos^2(\varphi_i)E\{\sin^2(n_i)\}\\
&\qquad +E\{\Delta x_i^2\}E\{\sin^2(\hat{\theta}_i)\}\\
&\qquad +E\{\Delta y_i^2\}E\{\cos^2(\hat{\theta}_i)\}\\
&\quad = d_i^2\cos^2(\varphi_i)\sigma_i^2+\sigma_{si}^2\\
&\quad = l_i^2\sigma_i^2+\sigma_{si}^2 \qquad (47)\\
&E\{\nu_i\nu_i\}\\
&\quad = E\{\{d_i[\cos(n_i)\cos(\varphi_i)\sin(\hat{\varphi}_i)-\cos(\hat{\varphi}_i)\sin(\varphi_i)]\\
&\qquad -[\Delta x_i\cos(\hat{\theta}_i)\sin(\hat{\varphi}_i)+\Delta y_i\sin(\hat{\theta}_i)\sin(\hat{\varphi}_i)\\
&\qquad -\Delta z_i\cos(\hat{\varphi}_i)]\}^2\}\\
&\quad = d_i^2E\{sin^2(\hat{\varphi}_i)\cos^2(\varphi_i)\cos^2(n_i)\\
&\qquad +\cos^2(\hat{\varphi}_i)\sin^2(\varphi_i)-1/2\sin(2\hat{\varphi}_i)\sin(2\varphi_i)\cos(n_i)\}\\
&\qquad +E\{\Delta x_i^2\}E\{\cos^2(\hat{\theta}_i)\sin^2(\hat{\varphi}_i)\}\\
&\qquad +E\{\Delta y_i^2\}E\{\sin^2(\hat{\theta}_i)\sin^2(\hat{\varphi}_i)\}\\
&\qquad +E\{\Delta z_i^2\}E\{(\cos^2(\hat{\varphi}_i)\}\\
&\quad = d_i^2(1/4\cos^2(\varphi_i)(1-E\{\cos(2\varphi_i+2\omega_i)\})\\
&\qquad \times(1+E\{\cos(2n_i)\})\\
&\qquad +1/2\sin^2(\varphi_i)(1+E\{\cos(2\varphi_i+2\omega_i)\})\\
&\qquad -1/2\sin(2\varphi_i)E\{\sin(2\varphi_i+2\omega_i)\}E\{\cos(n_i)\})\\
&\qquad +\sigma_{si}\\
&\quad = d_i^2\rho_i^2(1-\sigma_i^2\cos^2(\varphi_i))+\sigma_{si}^2\\
&\quad = \rho_i^2(d_i^2-\sigma_i^2l_i^2)+\sigma_{si}^2 \qquad (48)
\end{aligned}
$$

APPENDIX B

Let us directly calculate the expectation of $A^T WA$.

$$
\begin{aligned}
\Gamma &= E\{A^T WA\}\\
&= E\{[F \quad -h]^T W[F \quad -h]\}\\
&= E\{\begin{bmatrix} F^T WF & -F^T Wh\\ -(F^T Wh)^T & h^T Wh\end{bmatrix}\}\\
&= E\{\begin{bmatrix} Z_1 & -Z_2\\ -Z_2^T & Z_3\end{bmatrix}\} \qquad (49)
\end{aligned}
$$

where

$$
\begin{cases}
Z_1=\sum_{i=0}^{N-1} w_{1i}M_i^T\hat{J}_{1i}M_i+w_{2i}M_i^T\hat{J}_{2i}M_i\\
Z_2=\sum_{i=0}^{N-1} w_{1i}M_i^T\hat{J}_{1i}\hat{s}_i+w_{2i}M_i^T\hat{J}_{2i}\hat{s}_i\\
Z_3=\sum_{i=0}^{N-1} w_{1i}\hat{s}_i^T\hat{J}_{1i}\hat{s}_i+w_{2i}\hat{s}_i^T\hat{J}_{2i}\hat{s}_i
\end{cases} \qquad (50)
$$

where $\hat{J}_{1i}=\hat{b}_i\hat{b}_i^T$ and $\hat{J}_{2i}=\hat{c}_i\hat{c}_i^T$, $w_{1i}=1/(l_i^2\sigma_i^2+\sigma_{si}^2)$ and $w_{2i}=1/(\rho_i^2(d_i^2-\sigma_i^2l_i^2)+\sigma_{si}^2)$ are the diagonal elements of the weighting matrix W. Next we first calculate the value of J_{1i} and J_{2i} without errors in b_i and c_i.

$$
\begin{aligned}
J_{1i} &= \begin{bmatrix}\sin(\theta_i)\\ -\cos(\theta_i)\\ 0\end{bmatrix}\begin{bmatrix}\sin(\theta_i) & -\cos(\theta_i) & 0\end{bmatrix}\\
&= \begin{bmatrix}\sin^2(\theta_i) & -\sin(\theta_i)\cos(\theta_i) & 0\\ -\sin(\theta_i)\cos(\theta_i) & \cos^2(\theta_i) & 0\\ 0 & 0 & 0\end{bmatrix}\\
&= \begin{bmatrix}x_{1i}^0 & x_{2i}^0 & 0\\ x_{2i}^0 & x_{3i}^0 & 0\\ 0 & 0 & 0\end{bmatrix} \qquad (51)\\
J_{2i} &= \begin{bmatrix}\cos(\theta_i)\sin(\varphi_i)\\ \sin(\theta_i)\sin(\varphi_i)\\ -\cos(\varphi_i)\end{bmatrix}\begin{bmatrix}\cos(\theta_i)\sin(\varphi_i)\\ \sin(\theta_i)\sin(\varphi_i)\\ -\cos(\varphi_i)\end{bmatrix}^T\\
&= \begin{bmatrix}y_{1i}^0 & y_{2i}^0 & y_{3i}^0\\ y_{2i}^0 & y_{4i}^0 & y_{5i}^0\\ y_{3i}^0 & y_{5i}^0 & y_{6i}^0\end{bmatrix} \qquad (52)
\end{aligned}
$$

where

$$
\begin{cases}
y_{1i}^0=\cos^2(\theta_i)\sin^2(\varphi_i)\\
y_{2i}^0=\frac{1}{2}\sin(2\theta_i)\sin^2(\varphi_i)\\
y_{3i}^0=-\frac{1}{2}\cos(\theta_i)\sin(2\varphi_i)\\
y_{4i}^0=\sin^2(\theta_i)\sin^2(\varphi_i)\\
y_{5i}^0=-\frac{1}{2}\sin(\theta_i)\sin(2\varphi_i)\\
y_{6i}^0=\cos^2(\varphi_i)
\end{cases} \qquad (53)
$$

Now let us calculate the value of $\hat{J}_{1i}$ and $\hat{J}_{2i}$ with errors in $\hat{b}_i$ and $\hat{c}_i$.

$$
\begin{aligned}
\hat{J}_{1i} &= \begin{bmatrix}\sin(\hat{\theta}_i)\\ -\cos(\hat{\theta}_i)\\ 0\end{bmatrix}\begin{bmatrix}\sin(\hat{\theta}_i) & -\cos(\hat{\theta}_i) & 0\end{bmatrix}\\
&= \begin{bmatrix}x'_{1i} & x'_{2i} & 0\\ x'_{2i} & x'_{3i} & 0\\ 0 & 0 & 0\end{bmatrix} \qquad (54)\\
\hat{J}_{2i} &= \begin{bmatrix}\cos(\hat{\theta}_i)\sin(\hat{\varphi}_i)\\ \sin(\hat{\theta}_i)\sin(\hat{\varphi}_i)\\ -\cos(\hat{\varphi}_i)\end{bmatrix}\begin{bmatrix}\cos(\hat{\theta}_i)\sin(\hat{\varphi}_i)\\ \sin(\hat{\theta}_i)\sin(\hat{\varphi}_i)\\ -\cos(\hat{\varphi}_i)\end{bmatrix}^T\\
&= \begin{bmatrix}y'_{1i} & y'_{2i} & y'_{3i}\\ y'_{2i} & y'_{4i} & y'_{5i}\\ y'_{3i} & y'_{5i} & y'_{6i}\end{bmatrix} \qquad (55)
\end{aligned}
$$

where

$$
\begin{cases}
x'_{1i}=\sin^2(\theta_i)+\cos(2\theta_i)\sin^2(n_i)+\frac{1}{2}\sin(2\theta_i)\sin(n_i)\\
x'_{2i}=-\sin(\theta_i)\cos(\theta_i)+\sin(2\theta_i)\sin^2(n_i)\\
-\cos(2\theta_i)\sin(2n_i)\\
x'_{3i}=\cos^2(\theta_i)-\cos(2\theta_i)\sin^2(n_i)-\frac{1}{2}\sin(2\theta_i)\sin(n_i)
\end{cases} \qquad (56)
$$

$$\begin{cases} y'_{1i} = \cos^2(\hat{\theta}_i)\sin^2(\hat{\varphi}_i) \\ = [\cos^2(\theta_i) - \cos(2\theta_i)\sin^2(n_i) - \frac{1}{2}\sin(2\theta_i)\sin(n_i)]\cdot \\ [\sin^2(\varphi_i) + \cos(2\varphi_i)\sin^2(\omega_i) + \frac{1}{2}\sin(2\varphi_i)\sin(\omega_i)] \\ y'_{2i} = \frac{1}{2}\sin(2\hat{\theta}_i)\sin^2(\hat{\varphi}_i) \\ = [\frac{1}{2}\sin(2\theta_i) - \sin(2\theta_i)\sin^2(n_i) + \cos(2\theta_i)\sin(2n_i)]\cdot \\ [\sin^2(\varphi_i) + \cos(2\varphi_i)\sin^2(\omega_i) + \frac{1}{2}\sin(2\varphi_i)\sin(\omega_i)] \\ y^0_{3i} = -\frac{1}{2}\cos(\hat{\theta}_i)\sin(2\hat{\varphi}_i) \\ \approx [\cos(\theta_i) - \sin(\theta_i)\sin(n_i)]\cdot \\ [-\frac{1}{2}\sin(2\theta_i) + \sin(2\theta_i)\sin^2(n_i) - \cos(2\theta_i)\sin(2n_i)] \\ y'_{4i} = \sin^2(\hat{\theta}_i)\sin^2(\hat{\varphi}_i) \\ = [\sin^2(\theta_i) + \cos(2\theta_i)\sin^2(n_i) + \frac{1}{2}\sin(2\theta_i)\sin(n_i)] \\ [\sin^2(\varphi_i) + \cos(2\varphi_i)\sin^2(\omega_i) + \frac{1}{2}\sin(2\varphi_i)\sin(\omega_i)] \\ y'_{5i} = -\frac{1}{2}\sin(\hat{\theta}_i)\sin(2\hat{\varphi}_i) \\ \approx [\sin(\theta_i) + \cos(\theta_i)\sin(n_i)] \\ [-\frac{1}{2}\sin(2\theta_i) + \sin(2\theta_i)\sin^2(n_i) - \cos(2\theta_i)\sin(2n_i)] \\ y'_{6i} = \cos^2(\hat{\varphi}_i) \\ = [\cos^2(\varphi_i) - \cos(2\varphi_i)\sin^2(\omega_i) - \frac{1}{2}\sin(2\varphi_i)\sin(\omega_i)] \end{cases} \tag{57}$$

The expectation of matrices $\hat{J}_{1i}$ and $\hat{J}_{2i}$ is equivalent to the expectation of each element in matrices.

$$\begin{cases} E\{x'_{1i}\} = \sin^2(\theta_i) + \sigma_i^2\cos(2\theta_i) \\ E\{x'_{2i}\} = -\sin(\theta_i)\cos(\theta_i) + \sigma_i^2\sin(2\theta_i) \\ E\{x'_{3i}\} = \cos^2(\theta_i) - \sigma_i^2\cos(2\theta_i) \end{cases} \tag{58}$$

$$\begin{cases} E\{y'_{1i}\} = \cos^2(\theta_i)\sin^2(\varphi_i) - \sigma_i^2\cos(2\theta_i)\sin^2(\varphi_i) \\ +\rho_i^2\cos^2(\theta_i)\cos(2\varphi_i) \\ E\{y'_{2i}\} = \frac{1}{2}\sin(2\theta_i)\sin^2(\varphi_i) - \sigma_i^2\sin(2\theta_i)\sin^2(\varphi_i) \\ +\frac{\rho_i^2}{2}\sin(2\theta_i)\cos(2\varphi_i) \\ E\{y'_{3i}\} = -\frac{1}{2}\cos(\theta_i)\sin(2\varphi_i) + \frac{\sigma_i^2}{4}\cos(\theta_i)\sin(2\varphi_i) \\ +\rho_i^2\cos(\theta_i)\sin(2\varphi_i) \\ E\{y'_{4i}\} = \sin^2(\theta_i)\sin^2(\varphi_i) + \sigma_i^2\cos(2\theta_i)\sin^2(\varphi_i) \\ +\rho_i^2\sin^2(\theta_i)\cos(2\varphi_i) \\ E\{y'_{5i}\} = -\frac{1}{2}\sin(\theta_i)\sin(2\varphi_i) + \frac{\sigma_i^2}{4}\sin(\theta_i)\sin(2\varphi_i) \\ +\rho_i^2\sin(\theta_i)\sin(2\varphi_i) \\ E\{y'_{6i}\} = \cos^2(\varphi_i) - \rho_i^2\cos(2\varphi_i) \end{cases} \tag{59}$$

where • is the items that causes the bias. Obviously, we can estimate the moving target parameters more accurately without these items. In the above calculation, we ignored the product terms of σ_i^2 and ρ_i^2. And we used the following approximation.

$$\begin{aligned} E\{\sin^2(n_i)\} &= \sigma_i^2 \\ E\{\sin^2(\omega_i)\} &= \rho_i^2 \\ E\{\cos(n_i)\} &\approx 1 - \frac{\sigma_i^2}{2} \\ E\{\cos(\omega_i)\} &\approx 1 - \frac{\rho_i^2}{2} \\ E\{\cos(2n_i)\} &= 1 - 2\sigma_i^2 \\ E\{\cos(2\omega_i)\} &= 1 - 2\rho_i^2 \\ E\{\cos(2n_i)\} &= 1 - 2\sigma_i^2 \\ E\{\cos(2\omega_i)\} &= 1 - 2\rho_i^2 \\ E\{\cos(2\varphi_i + 2\omega_i)\} &= cos(2\varphi_i)(1 - 2\rho_i^2) \\ E\{\sin(2\varphi_i + 2\omega_i)\} &= sin(2\varphi_i)(1 - 2\rho_i^2) \end{aligned} \tag{60}$$

After the above analysis, we can easily get the equations

$$\begin{aligned} E\{\hat{\boldsymbol{J}}_{1i}\} &= \boldsymbol{J}_{1i} + \Delta\boldsymbol{J}_{1i} \\ E\{\hat{\boldsymbol{J}}_{2i}\} &= \boldsymbol{J}_{2i} + \Delta\boldsymbol{J}_{2i} \end{aligned} \tag{61}$$

where $\Delta\boldsymbol{J}_{1i}$ and $\Delta\boldsymbol{J}_{2i}$ are the bias terms. The bias terms of $\boldsymbol{Z}_1$ and $\boldsymbol{Z}_2$ are obtained as

$$\begin{cases} \Delta\boldsymbol{Z}_1 = \sum_{i=0}^{N-1} w_{1i}\boldsymbol{M}_i^T\Delta\boldsymbol{J}_{1i}\boldsymbol{M}_i + w_{2i}\boldsymbol{M}_i^T\Delta\boldsymbol{J}_{2i}\boldsymbol{M}_i \\ \Delta\boldsymbol{Z}_2 = \sum_{i=0}^{N-1} w_{1i}\boldsymbol{M}_i^T\Delta\boldsymbol{J}_{1i}S_i + w_{2i}\boldsymbol{M}_i^T\Delta\boldsymbol{J}_{2i}\boldsymbol{s}_i \end{cases} \tag{62}$$

Since there are position errors, the bias term of Z_3 cannot be easily obtained in this way. If the joint effect of position error and measurement error is ignored, it consists of two parts.

$$\Delta\boldsymbol{Z}_3 = \sum_{i=0}^{N-1} w_{1i}\boldsymbol{s}_i^T\Delta\boldsymbol{J}_{1i}S_i + w_{2i}\boldsymbol{s}_i^T\Delta\boldsymbol{J}_{2i}\boldsymbol{s}_i + \sum_{i=0}^{N-1} w_{1i}\sigma_{si}^2 + w_{2i}\sigma_{si}^2 \tag{63}$$

$E[\Psi]$ can be expressed as

$$E[\Psi] = \begin{bmatrix} \Delta\boldsymbol{Z}_1 & -\Delta\boldsymbol{Z}_2 \\ -\Delta\boldsymbol{Z}_2^T & \Delta\boldsymbol{Z}_3 \end{bmatrix} \tag{64}$$

APPENDIX C

The FIM of z is obtained as

$$\begin{aligned} \boldsymbol{\Omega}(z) &= E\{\left[(\boldsymbol{a}-\boldsymbol{a}_0)^T\boldsymbol{Q}_a^{-1}\frac{\partial\boldsymbol{a}_0}{\partial z^T} + (\hat{\boldsymbol{s}}-\boldsymbol{s})^T\boldsymbol{Q}_s^{-1}\frac{\partial\boldsymbol{s}}{\partial z^T}\right]^T \\ &\quad \left[(\boldsymbol{a}-\boldsymbol{a}_0)^T\boldsymbol{Q}_a^{-1}\frac{\partial\boldsymbol{a}_0}{\partial z^T} + (\hat{\boldsymbol{s}}-\boldsymbol{s})^T\boldsymbol{Q}_s^{-1}\frac{\partial\boldsymbol{s}}{\partial z^T}\right]\} \\ &= \left[\frac{\partial\boldsymbol{a}_0}{\partial z^T}\right]^T\boldsymbol{Q}_a^{-1}\frac{\partial\boldsymbol{a}_0}{\partial z^T} + \left[\frac{\partial\boldsymbol{s}}{\partial z^T}\right]^T\boldsymbol{Q}_s^{-1}\frac{\partial\boldsymbol{s}}{\partial z^T}. \end{aligned} \tag{65}$$

where $\frac{\partial \boldsymbol{a}_0}{\partial z^T} = \left[\frac{\partial \boldsymbol{a}_0}{\partial \boldsymbol{x}^T} \ \frac{\partial \boldsymbol{a}_0}{\partial \boldsymbol{s}^T}\right] = [\boldsymbol{G_x}, \boldsymbol{G_s}]$ and $\frac{\partial \boldsymbol{s}}{\partial z^T} = \left[\frac{\partial \boldsymbol{s}}{\partial \boldsymbol{x}^T} \ \frac{\partial \boldsymbol{s}}{\partial \boldsymbol{s}^T}\right] = \left[\boldsymbol{0}_{6N\times 3} \ \boldsymbol{I}_{3N\times 3N}\right]$, where

$$\boldsymbol{G}_x = \left[\frac{\partial \theta_0}{\partial \boldsymbol{x}}, \cdots, \frac{\partial \theta_{N-1}}{\partial \boldsymbol{x}}, \frac{\partial \varphi_0}{\partial \boldsymbol{x}}, \cdots, \frac{\partial \varphi_{N-1}}{\partial \boldsymbol{x}}\right]^T$$
$$\boldsymbol{G}_s = \left[\frac{\partial \theta_0}{\partial \boldsymbol{s}}, \cdots, \frac{\partial \theta_{N-1}}{\partial \boldsymbol{s}}, \frac{\partial \varphi_0}{\partial \boldsymbol{s}}, \cdots, \frac{\partial \varphi_{N-1}}{\partial \boldsymbol{s}}\right]^T, \quad (66)$$

where $\frac{\partial \theta_i}{\partial \boldsymbol{x}} = [\frac{\partial \theta_i}{\partial \boldsymbol{p}_0}; \frac{\partial \theta_i}{\partial \boldsymbol{v}}]$, $\frac{\partial \varphi_i}{\partial \boldsymbol{x}} = [\frac{\partial \varphi_i}{\partial \boldsymbol{p}_0}; \frac{\partial \varphi_i}{\partial \boldsymbol{v}}]$

$$\begin{cases} \frac{\partial \theta_i}{\partial \boldsymbol{p}_0} = [-\sin(\theta_i), \cos(\theta_i), 0]^T / l_i \\ \frac{\partial \varphi_i}{\partial \boldsymbol{p}_0} = [-\cos(\theta_i)\sin(\varphi_i), -\sin(\theta_i)\sin(\varphi_i), \cos(\varphi_i)]^T / d_i \\ \frac{\partial \theta_i}{\partial \boldsymbol{v}} = (i-1)T \frac{\partial \theta_i}{\partial \boldsymbol{p}_0} \\ \frac{\partial \varphi_i}{\partial \boldsymbol{v}} = (i-1)T \frac{\partial \varphi_i}{\partial \boldsymbol{p}_0} \\ \frac{\partial \theta_i}{\partial \boldsymbol{s}} = [\boldsymbol{0}_{1\times 3i}, \sin(\theta_i), -\cos(\theta_i), 0, \boldsymbol{0}_{1\times 3(N-i-1)}]^T / l_i \\ \frac{\partial \theta_i}{\partial \boldsymbol{s}} = [\boldsymbol{0}_{1\times 3i}, \cos(\theta_i)\sin(\varphi_i), \sin(\theta_i) sin(\varphi_i), \\ -cos(\varphi_i), \boldsymbol{0}_{1\times 3(N-i-1)}]^T / d_i \end{cases} \quad (67)$$

Rewritten Eq.(65) as

$$\boldsymbol{\Omega}(z) = \begin{bmatrix} \boldsymbol{Y}_1 & \boldsymbol{Y}_2 \\ \boldsymbol{Y}_2^T & \boldsymbol{Y}_3 \end{bmatrix}, \quad (68)$$

where $\boldsymbol{Y}_1 = \boldsymbol{G_x}^T \boldsymbol{Q}_a^{-1} \boldsymbol{G_x}$, $\boldsymbol{Y}_2 = \boldsymbol{G_x}^T \boldsymbol{Q}_a^{-1} \boldsymbol{G_s}$ and $\boldsymbol{Y}_3 = \boldsymbol{G_s}^T \boldsymbol{Q}_a^{-1} \boldsymbol{G_s} + \boldsymbol{Q}_s^{-1}$, where $\boldsymbol{G_x} = \frac{\partial \boldsymbol{a}_0}{\partial \boldsymbol{x}^T}$ and $\boldsymbol{G_s} = \frac{\partial \boldsymbol{a}_0}{\partial \boldsymbol{s}^T}$.

REFERENCES

[1] X. Wu, W.-P. Zhu, and J. Yan, "A high-resolution DOA estimation method with a family of nonconvex penalties," *IEEE Trans. Veh. Technol.*, vol. 67, no. 6, pp. 4925–4938, Jun. 2018.

[2] X. Wang, L. Wan, M. Huang, C. Shen, and K. Zhang, "Polarization channel estimation for circular and non-circular signals in massive MIMO systems," *IEEE J. Sel. Topics Signal Process.*, vol. 13, no. 5, pp. 1001–1016, Sep. 2019.

[3] X. Wang, W. Wang, J. Liu, X. Li, and J. Wang, "A sparse representation scheme for angle estimation in monostatic MIMO radar," *Signal Process.*, vol. 104, pp. 258–263, Nov. 2014.

[4] B. Yao, W. Wang, W. Han, and Q. Yin, "Distributed angle estimation by multiple frequencies synthetic array in wireless sensor localization system," *IEEE Trans. Wireless Commun.*, vol. 13, no. 2, pp. 876–887, Feb. 2014.

[5] W. Zhang, Q. Yin, H. Chen, F. Gao, and N. Ansari, "Distributed angle estimation for localization in wireless sensor networks," *IEEE Trans. Wireless Commun.*, vol. 12, no. 2, pp. 527–537, Feb. 2013.

[6] Q. Zhou and Z. Duan, "Weighted intersections of bearing lines for AOA based localization," in *Proc. 17th Int. Conf. Inf. Fusion*, Jul. 2014, pp. 1–8.

[7] A. N. Bishop, B. D. O. Anderson, B. Fidan, P. N. Pathirana, and G. Mao, "Bearing-only localization using geometrically constrained optimization," *IEEE Trans. Aerosp. Electron. Syst.*, vol. 45, no. 1, pp. 308–320, Jan. 2009.

[8] X. Wang, L. Wang, X. Li, and G. Bi, "Nuclear norm minimization framework for DOA estimation in MIMO radar," *Signal Process.*, vol. 135, pp. 147–152, Jun. 2017.

[9] E. Tzoreff and A. J. Weiss, "Path design for best emitter location using two mobile sensors," *IEEE Trans. Signal Process.*, vol. 65, no. 19, pp. 5249–5261, Oct. 2017.

[10] J. Ousingsawat and M. E. Campbell, "On-line estimation and path planning for multiple vehicles in an uncertain environment," *Int. J. Robust Nonlinear Control*, vol. 14, no. 8, pp. 741–766, May 2004.

[11] J. E. L. Cadre and C. Jauffret, "Discrete-time observability and estimability analysis for bearings-only target motion analysis," *IEEE Trans. Aerosp. Electron. Syst.*, vol. 33, no. 1, pp. 178–201, Jan. 1997.

[12] F. Wen, X. Xiong, J. Su, and Z. Zhang, "Angle estimation for bistatic MIMO radar in the presence of spatial colored noise," *Signal Process.*, vol. 134, pp. 261–267, May 2017.

[13] W. Ding, Z. Li, and Y. Wu, "Constrained total least squares algorithm for passive location based on bearing-only measurements," *Sci. China F, Inf. Sci.*, vol. 50, no. 4, pp. 576–586, 2007.

[14] K. C. Ho and Y. T. Chan, "An asymptotically unbiased estimator for bearings-only and Doppler-bearing target motion analysis," *IEEE Trans. Signal Process.*, vol. 54, no. 3, pp. 809–822, Mar. 2006.

[15] K. Doğançay, "On the bias of linear least squares algorithms for passive target localization," *Signal Process.*, vol. 84, no. 3, pp. 475–486, Mar. 2004.

[16] X. Wu, W.-P. Zhu, J. Yan, and Z. Zhang, "Two sparse-based methods for off-grid direction-of-arrival estimation," *Signal Process.*, vol. 142, pp. 87–95, Jan. 2018.

[17] W. H. Foy, "Position-location solutions by Taylor-series estimation," *IEEE Trans. Aerosp. Electron. Syst.*, vol. AES-12, no. 2, pp. 187–194, Mar. 1976.

[18] A. G. Lingren and K. F. Gong, "Position and velocity estimation via bearing observations," *IEEE Trans. Aerosp. Electron. Syst.*, vol. AES-14, no. 4, pp. 564–577, Jul. 1978.

[19] Y. T. Chan and S. W. Rudnicki, "Bearings-only and Doppler-bearing tracking using instrumental variables," *IEEE Trans. Aerosp. Electron. Syst.*, vol. 28, no. 4, pp. 1076–1083, Oct. 1992.

[20] S. Nardone, A. Lindgren, and K. Gong, "Fundamental properties and performance of conventional bearings-only target motion analysis," *IEEE Trans. Autom. Control*, vol. AC-29, no. 9, pp. 775–787, Sep. 1984.

[21] V. J. Aidala and S. C. Nardone, "Biased estimation properties of the pseudolinear tracking filter," *IEEE Trans. Aerosp. Electron. Syst.*, vol. AES-18, no. 4, pp. 432–441, Jul. 1982.

[22] K. Doğançay, "Passive emitter localization using weighted instrumental variables," *Signal Process.*, vol. 84, no. 3, pp. 487–497, Mar. 2004.

[23] K. Dogancay and G. Ibal, "Instrumental variable estimator for 3D bearings-only emitter localization," in *Proc. Int. Conf. Intell. Sensors, Sensor Netw. Inf. Process.*, Dec. 2005, pp. 63–68.

[24] L. Badriasl and K. Dogancay, "Three-dimensional target motion analysis using azimuth/elevation angles," *IEEE Trans. Aerosp. Electron. Syst.*, vol. 50, no. 4, pp. 3178–3194, Oct. 2014.

[25] H. Wang, L. Wan, M. Dong, K. Ota, and X. Wang, "Assistant vehicle localization based on three collaborative base stations via SBL-based robust DOA estimation," *IEEE Internet Things J.*, vol. 6, no. 3, pp. 5766–5777, Jun. 2019.

[26] Y. Wang and K. C. Ho, "An asymptotically efficient estimator in closed-form for 3-D AOA localization using a sensor network," *IEEE Trans. Wireless Commun.*, vol. 14, no. 12, pp. 6524–6535, Dec. 2015.

[27] B. R. Geiger, J. F. Horn, A. M. Delullo, L. N. Long, and A. F. Niessner, "Optimal path planning of UAVs using direct collocation with nonlinear programming," in *Proc. AIAA Guid., Navigat., Control Conf. Exhibit*, Aug. 2006, p. 6199.

[28] K. Doğançay and H. Hmam, "Optimal angular sensor separation for AOA localization," *Signal Process.*, vol. 88, pp. 1248–1260, May 2008.

[29] K. Doğançay and H. Hmam, "On optimal sensor placement for time-difference-of-arrival localization utilizing uncertainty minimization," in *Proc. 17th Eur. Signal Process. Conf.*, Aug. 2009, pp. 1136–1140.

[30] S. M. Kay, "Fundamentals of statistical signal processing: Estimation theory," *Technometrics*, vol. 37, no. 4, pp. 465–466, 1993.

[31] J. M. Passerieux and D. Van Cappel, "Optimal observer maneuver for bearings-only tracking," *IEEE Trans. Aerosp. Electron. Syst.*, vol. 34, no. 3, pp. 777–788, Jul. 1998.

[32] Y. Oshman and P. Davidson, "Optimization of observer trajectories for bearings-only target localization," *IEEE Trans. Aerosp. Electron. Syst.*, vol. 35, no. 3, pp. 892–902, Jul. 1999.

[33] M. L. Hernandez, "Optimal sensor trajectories in bearings-only tracking," in *Proc. 7th Int. Conf. Inf. Fusion*, vol. 2, 2004, pp. 893–900.

[34] B. Grocholsky, A. Makarenko, and H. Durrant-Whyte, "Information-theoretic coordinated control of multiple sensor platforms," in *Proc. IEEE Int. Conf. Robot. Autom.*, vol. 1, Sep. 2003, pp. 1521–1526.

[35] K. Doğançay, "UAV path planning for passive emitter localization," *IEEE Trans. Aerosp. Electron. Syst.*, vol. 48, no. 2, pp. 1150–1166, Apr. 2012.

[36] D.-C. Chang and M.-W. Fang, "Bearing-only maneuvering mobile tracking with nonlinear filtering algorithms in wireless sensor networks," *IEEE Syst. J.*, vol. 8, no. 1, pp. 160–170, Mar. 2014.

[37] Z. Ma and K. C. Ho, "A study on the effects of sensor position error and the placement of calibration emitter for source localization," *IEEE Trans. Wireless Commun.*, vol. 13, no. 10, pp. 5440–5452, Oct. 2014.

LANG HE received the B.S. degree from the Electronic Engineering Department, Nanjing University of Aeronautics and Astronautics, China, in 2017, where he is currently pursuing the M.S. degree. His research interests include signal and information processing and radiation source localization.

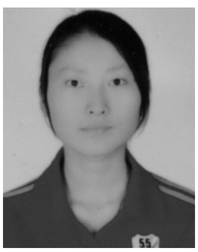

PAN GONG received the M.S. degree from Yunnan Minzu University, Yunnan, China, in 2016. She is currently pursuing the Ph.D. degree with the Electronic Engineering Department, Nanjing University of Aeronautics and Astronautics. Her research interests include array signal processing and communication signal processing.

XIAOFEI ZHANG received the M.S. degree from Wuhan University, Wuhan, China, in 2001, and the Ph.D. degree in communication and information systems from the Nanjing University of Aeronautics and Astronautics, Nanjing, China, in 2005.

He is currently a Full Professor with the Electronic Engineering Department, Nanjing University of Aeronautics and Astronautics, and a member of the Key Laboratory of Dynamic Cognitive System of Electromagnetic Spectrum Space, Ministry of Industry and Information Technology, Nanjing University of Aeronautics and Astronautics. His research interests include array signal processing and communication signal processing.

Prof. Zhang serves on the Technical Program Committees of The IEEE 2010 International Conference on Wireless Communications and Signal Processing (WCSP 2010), The IEEE 2011 International Conference on Wireless Communications and Signal Processing (WCSP 2011), ssme2010, and 2011 International Workshop on Computation Theory and Information Technology. He also serves as an Editor for the *International Journal of Digital Content Technology and its Applications* (JDCTA), the *International Journal of Technology and Applied Science* (IJTAS), the *Journal of Communications and Information Sciences*, the *Scientific Journal of Microelectronics*, and the *International Journal of Information Engineering* (IJIE). He also serves regularly as a peer-reviewer for the IEEE Transactions on Wireless Communication, the IEEE Transactions on Vehicular Technology, the *Journal on Advances in Signal Processing* (EURASIP), the IEEE Communications Letters, *Signal Processing*, the *International Journal of Electronics*, the *International Journal of Communication Systems*, and *Wireless Communications and Mobile Computing*.

ZHENG WANG received the B.S. degree in electronic and information engineering from the Nanjing University of Aeronautics and Astronautics (NUAA), Nanjing, China, in 2009, the M.S. degree in communications from the Department of Electrical and Electronic Engineering, University of Manchester, Manchester, U.K., in 2010, and the Ph.D. degree in communication engineering from the Imperial College London, U.K., in 2015.

From 2015 to 2016, he served as a Research Associate with the Imperial College London. From 2016 to 2017, he was a Senior Engineer with the Radio Access Network Research and Development Division, Huawei Technologies Company. He is currently an Assistant Professor with the College of Electronic and Information Engineering, NUAA. His current research interests include lattice methods for wireless communications, cognitive radio, and physical layer security.